Broadband tuning of a long-cavity all-fiber mode locked Thulium-doped fiber laser using an acousto-optic bandpass filter

E. Hernández-Escobar,[1] M. Bello-Jiménez,[1]* A. Camarillo-Avilés,[1] R. López-Estopier,[1,2] O. Pottiez,[3] M. V. Hernández-Arriaga,[4] M. Durán-Sánchez,[2,5] B. Ibarra-Escamilla[5] and M. V. Andrés[6]

[1]*Instituto de Investigación en Comunicación Óptica (IICO), Universidad Autónoma de San Luis Potosí, Av. Karakorum No. 1470 Lomas 4ª Secc., 78210 San Luis Potosí, Mexico*
[2]*Consejo Nacional de Ciencia y Tecnología (CONACYT), Av. Insurgentes Sur No. 1582, Col. Crédito Constructor, Del. Benito Juárez, México, D.F. 039040, Mexico*
[3]*Centro de Investigaciones en Óptica (CIO), Loma del Bosque No. 115, Col. Lomas del Campestre, León, Guanajuato 37150, Mexico*
[4]*Instituto Tecnológico Superior de Rioverde, Carretera Rioverde-San Ciro km. 4.5, 79610 Rioverde, San Luis Potosí, Mexico*
[5]*Instituto Nacional de Astrofísica, Óptica y Electrónica (INAOE), Luis Enrique Erro No 1, Departamento de Óptica, 72000 Puebla, Mexico*
[6]*Universidad de Valencia, Departamento de Física Aplicada y Electromagnetismo, ICMUV, c/Dr. Moliner 50, Burjassot, 46100 Valencia, Spain*
**Corresponding author: miguel.bello@uaslp.mx*

Received XX Month XXXX; revised XX Month, XXXX; accepted XX Month XXXX; posted XX Month XXXX (Doc. ID XXXXX); published XX Month XXXX

A long-cavity passively mode-locked thulium-doped all-fiber laser is reported incorporating a tapered acousto-optic tunable bandpass filter (AOTBF). The operation of the AOTBF relies on the intermodal coupling between core and cladding modes when a flexural acoustic wave propagates along an 80-μm tapered fiber. The filter works in transmission and exhibits a 3-dB bandwidth of 9.02 nm with an insertion loss of 3.4 dB. The laser supports ultrashort pulse generation at a low repetition rate of 784.93 kHz. Optical pulses with 2.43 nm of optical bandwidth and 2.1 ps pulse duration were obtained in a broad tuning range from 1824.77 to 1905.16 nm.

http://dx.doi.org/10.1364/OL.99.099999

Mode-locked fiber lasers (MLFLs) have received a great deal of attention in the past years because of their capability to generate short or ultrashort optical pulses featuring low repetition rates [1-7]. For applications that require ultrashort optical pulses and sub-megahertz repetition rates, one of the most common scheme relies on the use of pulse picker devices [8-11], but this method introduces significant losses and increases the laser complexity. For this reason, the development of long-cavity all-fiber approaches have emerged as an alternative solution to overcome these drawbacks.

In the framework of MLFLs, passive configurations possess the advantage of generating the shortest optical pulses, but in a long-cavity scheme –i.e., lasers with a cavity length from a few hundreds of meters to several kilometers– the generation of wave-breaking free optical pulses becomes a difficult task. Therefore, the development of all-fiber elements with capacity to provide a robust and stable laser performance is an issue of particular interest. Following this research line, in-fiber acousto-optic (AO) devices based on flexural acoustic waves have been proposed and demonstrated as efficient bandpass filters that can work in transmission [12-15]. Among these approaches, our group has proposed an acousto-optic tunable bandpass filter (AOTBF) that uses a tiny section of coreless optical fiber as a core-mode blocker (CMB) [14,16,17], and generates no frequency shift. Now, and because of the growing interest in developing broad-bandwidth all-fiber devices, an improved AOTBF is presented based on the inclusion of a tapered optical fiber. The versatility of this AO device is demonstrated near the 2 microns region as a wavelength selective element in a thulium-doped fiber laser (TDFL).

The bandpass characteristics of the AOTBF are analyzed after the inclusion of an 80-μm tapered optical fiber. Experimental results show a reasonably wide (56.29 nm) and deep (22.2 dB) attenuation notch for the CMB, and the tapered AOTBF exhibits a 3-dB bandpass transmission bandwidth of 9.02 nm. This result is at least 9 times broader than the one obtained with a non-tapered fiber [14]. The filter capabilities are investigated in a long-cavity passively mode-locked TDFL, showing that ultrashort pulse

generation is supported by our setup. These results, to the best of our knowledge, are the first results describing an in-fiber AO tunable bandpass filter that fulfills the requirements of broadband operation and stable single ultrashort pulse generation in a long-cavity fiber laser (repetition rate < 1 MHz).

A schematic view of the AO tunable bandpass filter is shown in Fig. 1. A radio frequency (RF) source is used to drive a 20-mm piezoelectric disk (PD) and the acoustic vibrations are concentrated into an uncoated section of a tapered optical fiber through the tip of the aluminum horn. The section L of fiber, where acousto-optic interaction takes place, is composed of three segments of fiber labeled L_1, d and L_2. The length of section L_1 is selected to allow the LP_{01} mode to be coupled to a cladding mode previous to the CMB. The CMB, composed of a tiny section d of coreless optical fiber (Thorlabs FG125LA), is designed to strongly attenuate the optical wavelengths that remain guided by the fundamental mode because they do not fulfill the phase-matching condition. In this way, only the resonant wavelengths are capable to bypass the CMB via cladding propagation. After that, the cladding mode is coupled back to the core mode by the AO effect along the section of fiber L_2. This section L_2 is longer than L_1 in order to counterbalance the attenuation of the acoustic wave and maximize the transmittance [14]. The acoustic wave is damped at both ends of the filter structure in order to prevent unwanted acoustic reflections. With the purpose to improve the bandpass characteristics of the filter device, a double-ended tapered fiber is included. The tapered fiber will increase the acoustic intensity by reducing the cross section of the fiber. At the same time, it enhances the coupling coefficient by increasing the overlap between optical modes and acoustic perturbation that results from the expansion of the LP_{01} mode as the fiber diameter is reduced. One further advantage of using a tapered fiber is the linewidth increase of the acousto-optic resonance due to the specific perturbation introduced in the dispersion curves of the optical modes [18], which is of particular interest in the present work.

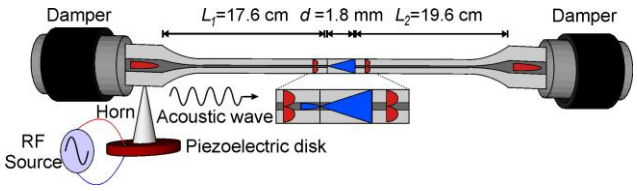

Fig. 1. Experimental arrangement of the AOTBF with tapered optical fiber.

The tapered fiber was prepared using a standard fusion and pulling technique, in which an oscillating flame comprised of a controlled mixture of oxygen and butane is used to soften the fiber. The fibers that compose the filter structure were initially tapered down to 80 μm in diameter, and subsequently spliced to form the filter arrangement. This fiber diameter ensures a reasonably broad spectral AO response [18] and easy manipulation with standard fiber-optic equipment. The lengths of the tapered sections L_1 and L_2 are 17.6 and 19.6 cm, respectively, both of them exhibiting a long decaying-exponential transition profile of 6.7 cm in length. The CMB, located in between fibers L_1 and L_2, has a length d of 1.8 mm. This length produces that light leaving section of fiber L_1 will be expanded over the front face of the fiber L_2 in the 1850 nm region. The total length L of the tapered fiber, including L_1, CMB and L_2 sections is 37.38 cm.

Figure 2(a) shows the transmittance spectrum of the CMB in the absence of acoustic wave. The CMB produces an attenuation notch of –22.2 dB at 1815.13 nm, providing a 56.29-nm attenuation band with at least 10 dB over a range of wavelengths from 1782.61 to 1838.9 nm. This result, which is narrower and less deep than the one obtained with a non-tapered fiber [14], could be attributed to the expansion of the fundamental mode as a result of tapering, leading to an increase of the effective mode area, which in turn favors the transmission of light through the CMB. Notwithstanding, the 80-μm taper produces a reasonably wide (56.29 nm) and deep (22.2 dB) attenuation notch for the CMB. Fig. 2(b) illustrates the bandpass characteristics of the AOTBF when an acoustic signal of 108.868 kHz and 32 V (hereinafter the voltage is a peak-to-peak measurement) is applied to the piezoelectric disk. The filter exhibits a 3-dB bandwidth of 9.02 nm and a minimum insertion loss of 3.4 dB at the resonant optical wavelength (λ_R) of 1816.2 nm. This last result is in agreement with the reported 3-dB stopband bandwidth (9.2 nm) for an 80 μm tapered fiber [18], and demonstrates the potential of tapered AOTBF to achieve a broad bandwidth transmission response. The calibration of the tapered AOTBF, the shift of resonant wavelength versus the acoustic wave frequency, is depicted in Fig. 2(c); a rate of change of –0.363 kHz/nm is measured in the wavelength region from 1765.3 to 1873.53 nm. This experimental slope could be estimated theoretically after a precise fiber characterization [19].

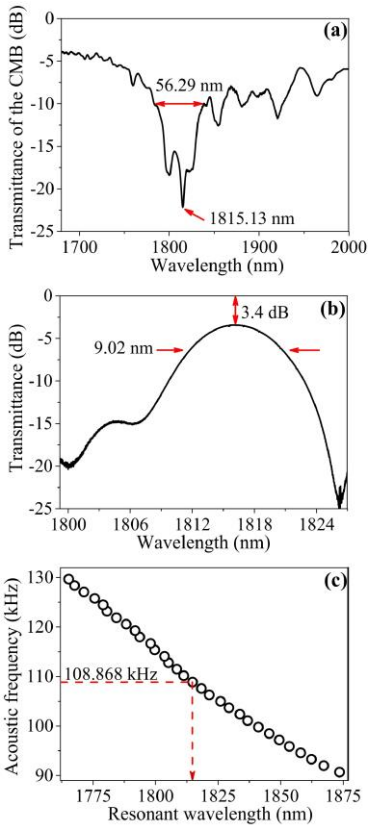

Fig. 2. Transmission characteristics of the AOTBF using a 37.4 cm long tapered fiber. (a) Transmittance of the CMB in the absence of acoustic wave, (b) Transmittance of the filter at the acoustic frequency of 108.868 kHz. (c) Shift of the resonant optical wavelength versus acoustic frequency. The dashed line shows the strongest intermodal coupling.

The filter capacities are investigated in a long-cavity passively mode-locked thulium-doped fiber laser. The experimental arrangement of the all-fiber laser is shown in Fig. 3. A fiber laser source emitting at 1567.64 nm is used to pump a 3-m long thulium-doped fiber (TDF, CorActive SCF-TM-8/125) with a maximum pump power of 1.73 W via the 1550/2000-nm wavelength division multiplexer (WDM). The length of the active fiber was chosen in order to optimize the continuous-wave (CW) power efficiency [20]. Then, and following a counterclockwise direction, the WDM is connected to a 50/50 fiber coupler. One output port of the coupler provides the laser output and the remaining coupler port is spliced to an in-line polarization controller (PC1) and the tapered AOTBF. The transmission port of the filter is spliced to the input port of a fiber-based polarization-dependent isolator (PD-ISO), which is connected in between two in-line polarization controllers, PC2 and PC3. The inclusion of a fiber delay line, 237 m of Thorlabs SM-2000 fiber, was necessary in order to benefit from the nonlinear polarization rotation effect (NPR) and to make the cavity long enough to achieve a repetition rate below 1 MHz. By properly adjusting PC2 and PC3 in the system, a stable mode-locking operation is generated.

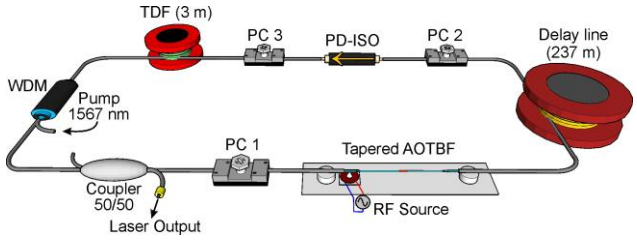

Fig. 3. Schematic of the NPR mode-locked thulium-doped all-fiber laser.

Initial measurements were performed in the CW regime. Figure 4(a) shows the cw operation when an acoustic signal of 108.868 kHz and 32.4 V is applied to the PD. The laser emission is located at 1813.85 nm, in agreement with the calibration of the tapered AOTBF. The cw laser line exhibits a 3-dB bandwidth of 50 pm, this value is the limit resolution of the OSA (Yokogawa AQ6375), thus, a narrower laser linewidth should be expected. At the noise floor level a reasonably broad ASE background of around 3.5 nm is observed as a result of the broadband transmission response of the filter. Figure 4(b) illustrates the tunable cw operation at different acoustic frequencies. The acoustic frequency was varied in a range between 126.768 and 88.358 kHz, which corresponds to a wavelength tuning range from 1771.87 to 1877.40 nm, respectively, achieving a broad tuning range of 105.53 nm. This tuning range could be re-adjusted by changing the length of active fiber [20]. For the presented set of measurements, laser emission was fixed to a peak power value of 0 dBm in the spectrum by adjusting the pump power, maintaining a signal-to-noise ratio (SNR) higher than 40 dB in all cases, and compensating for the changes of overall losses of the cavity for different wavelengths. Notwithstanding, the laser can reach a maximum output power of 219.4 mW by applying the maximum pump power (1.73 W).

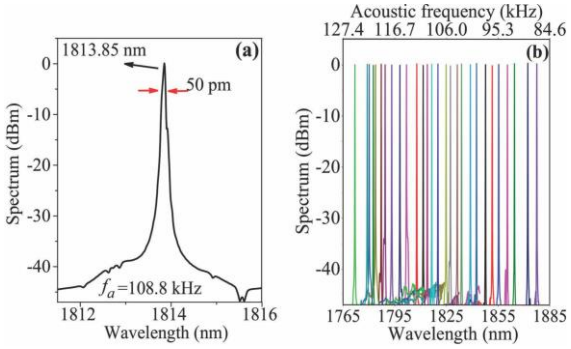

Fig. 4. Characteristics of the cw emission. (a) Measured optical spectrum of the laser at the acoustic frequency of 108.868 kHz. (b) Tunable operation: spectra at different acoustic frequencies.

By adjusting properly the polarization controllers, the laser is switched to a stable mode-locked (ML) pulse regime. Figure 5(a) shows the spectrum of ML emission at a pump power of 552 mW and applying an acoustic frequency of 91.718 kHz to the AOTBF. The spectrum is centered at 1864.45 nm and the 3-dB optical bandwidth is measured as 2.43 nm. Assuming a Gaussian pulse shape, it corresponds to a transform limited pulse duration of 2.1 ps. In order to confirm this estimation of the pulse duration, we have carried out an experimental characterization using a standard temporal pulse stretching technique. After propagation in a 750 m long SMF-28 fiber, with a dispersion of −67 ps^2/km at 1.9 μm [21], we obtained the pulse depicted in Fig. 5(b) that was measured using a 12.5-GHz photodetector (Newport 818-BB-51F) and a 20-GHz real-time oscilloscope (Tektronix DPO72004C). A full width at half maximum of 60 ps was measured, in good agreement with the expected value of 66.5 ps. The inset in Fig. 5(b) shows the train of ML pulses with a pulse interval T of 1.27 μs, which corresponds to the fundamental cavity round-trip time of a 264-m long cavity.

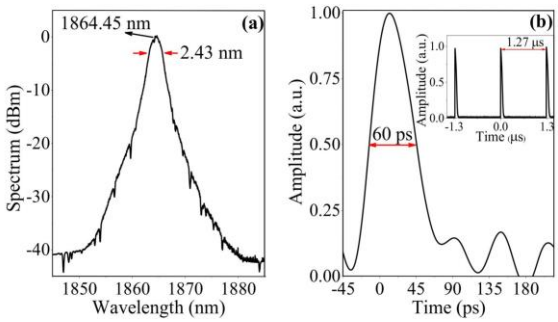

Fig. 5. Characteristics of the mode-locked pulse emission. (a) Measured optical spectrum of the laser at the acoustic frequency of 91.718 kHz. (b) Measurement of the stretched pulse after propagation in SMF-28 coil of 750-m. The inset shows the train of ML pulses with a pulse interval equal to 1.27 μs.

The corresponding RF spectrum is shown in Fig. 6(a), measured with a span of 40 kHz and resolution bandwidth of 10 Hz. It reveals a single peak located at the fundamental repetition frequency of 784.93 kHz and exhibits a SNR of 50 dB, indicating low-amplitude fluctuation. The absence of additional components on both sides of the fundamental peak suggests a stable and single-pulse ML operation. Figure 6(b) shows the average output power as a function of the pump power. The laser output increases linearly

after reaching the threshold of 328 mW, showing a slope efficiency of 18 %. Continuous wave operation is observed in a range between 328 and 403 mW. Beyond this interval the laser operates in a ML pulse regime. A maximum average output power of 261.5 mW is achieved when applying the highest pump power. A maximal pulse energy of 333 nJ is estimated according to the repetition rate of 784.93 kHz.

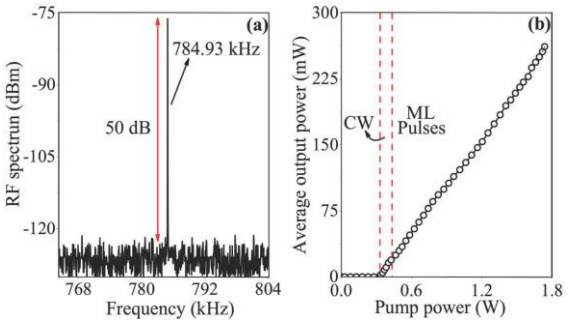

Fig. 6. (a) RF spectrum of the output pulse train measured with 40 kHz span and 10 Hz resolution bandwidth. (b) Average output power at different pump power conditions.

Tunable ML operation at different acoustic frequencies is demonstrated in Fig. 7(a). The acoustic frequency was varied between 104.238 and 82.206 kHz, which corresponds to a wavelength tuning range from 1824.77 to 1905.16 nm, respectively, obtaining a wide tuning operation interval of 80.39 nm. As in CW operation, the pump power was readjusted for each frequency in order to keep the emission constant at 0 dBm. The dependence of the laser fundamental frequency ($f_{rep} = 1/T$) as a function of the acoustic wave frequency (f_a) and the corresponding laser wavelength is also illustrated in Fig. 7(b). From this experimental plot, we can determine the actual net dispersion of the laser cavity. The average ratio $\Delta T/\Delta\lambda$ is equal to 9.95 ps/nm and gives a net dispersion of –18.3 ps^2 –i. e., $(\Delta T/\Delta\lambda)\times\lambda^2/(2\pi c)$– at the central wavelength of 1864.45 nm. Since the overall length of the cavity is 264 m, we can calculate the average chromatic dispersion of the cavity D = 37.7 ps/(nm-km). This cavity dispersion is mainly attributed to the long delay line of SM-2000 fiber used in our setup.

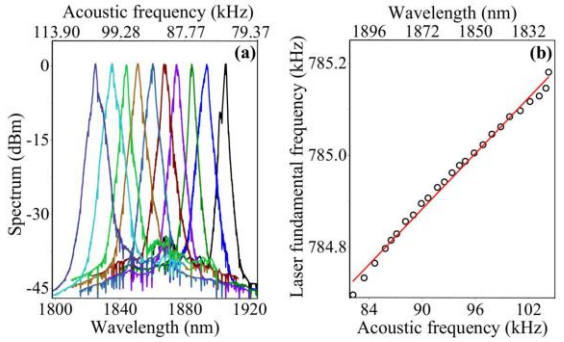

Fig. 7. (a) Tunable ML operation: spectra at different acoustic frequencies. (b) Dependence of the laser fundamental frequency as a function of the acoustic wave frequency and the laser wavelength.

In conclusion, we have demonstrated a broadband-tunable 2-microns mode-locked fiber laser. The laser cavity has an all-fiber configuration and is based on an improved in-fiber AOTBF incorporating a tapered optical fiber. The merits of the tapered AOTBF are a broad bandpass transmission bandwidth of 9.02 nm, which is an order of magnitude broader than the one obtained with a non-tapered fiber (~1 nm), a wide tuning range higher than 100 nm, and a reasonably low insertion loss of 3.4 dB. In addition, when the laser is operated in cw, the AOTBF permits a wide tuning range of 105.53 nm extending from 1771.87 to 1877.40 nm. In the ML regime, the AOTBF does not introduce any frequency shift and is capable to support the generation of a stable train of ML pulses at sub-megahertz repetition rate (~784 kHz). Optical pulses with 2.43 nm optical bandwidth and estimated pulse duration of about 2.1 ps were generated within a broad tuning range from 1824.77 to 1905.16 nm, and a maximum average output power of 261.5 mW. These results could be considered as the first demonstration of a tapered in-fiber AOTBF fulfilling the requirements of tunable, broad bandwidth operation, and stable ultrashort pulse generation in a long-cavity configuration.

Funding. CONACyT "Fronteras de la Ciencia" Grant 2438. M. V. Hernández-Arriaga is supported by TecNM project 5833.19-P.

References

1. X. H. Li, X. M. Liu, X. H. Hu, L. R. Wang, H. Lu, Y. S. Wang, and W. Zhao, Opt. Lett. **35**, 3249 (2010).
2. J. Chen, D. F. Jia, Y. C. Wu, C. L. Wang, Z. Y. Wang, and T. X. Yang, Chin. Phys. Lett. **28**, 114203 (2011).
3. B. N. Nyushkov, A. V. Ivanenko, S. M. Kobtsev, S. K. Turitsyn, C. Mou, L. Zhang, V. I. Denisov, and V. S. Pivtsov, Laser Phys. Lett. **9**, 59 (2012).
4. S. Boivinet, J.-B. Lecourt, Y. Hernandez, A. Fotiadi, M. Wuilpart, and P. Mégret, IEEE Photonics Technol. Lett. **26**, 2256 (2014).
5. Z. Mingfei, S. Haiyue, L. Tongling, and H. Kun, Quantum Electron. **47**, 877 (2017).
6. S. M. Ou, G. Y. Liu, L. Guo, Z. G. Zhang and Q. M. Zhang, Appl. Opt. **57**, 5068 (2018).
7. D. Jia, Y. Jin, X. Sun, Z. Li, Z., C. Ge, and Z. Wang, In 2018 Asia Communications and Photonics Conference (ACP) (pp. 1-3). IEEE (2018).
8. Y. Zaouter, L. Daniault, M. Hanna, D. N. Papadopoulos, F. Morin, C. Hönninger, F. Druon, E. Mottay, and P. Georges, Opt. Lett. **37**, 1460 (2012).
9. G. Sobon, P. Kaczmarek, A. Gluszek, J. Sotor, and K. M. Abramski, Opt. Commun. **347**, 8 (2015).
10. Z. Zhao and Y. Kobayashi, Appl. Phys. Express **9**, 012701 (2016).
11. S. Han, H. Jang, S. Kim, Y. J. Kim, S. W. Kim, Laser Phys. Lett. **14**, 080002 (2017).
12. K. J. Lee, D. I. Yeom, and B. Y. Kim, Opt. Express **15**, 2987 (2007).
13. C. Cuadrado-Laborde, M. Bello-Jiménez, A. Díez, J. L. Cruz, and M. V. Andrés, Opt. Lett. **39**, 68 (2014).
14. G. Ramírez-Meléndez, M. Bello-Jiménez, O. Pottiez, and M. V. Andrés, IEEE Photonics Tech. L. **29**, 1015 (2017).
15. L. Huang, W. Zhang, Y. Li, H. Han, X. Li, P. Chang, F. Gao, G. Zhang, L. Gao, and T. Zhu, Opt. Lett. **43**, 5431 (2018).
16. M. Bello Jiménez, E. Hernández Escobar, A. Camarillo Avilés, O. Pottiez, A. Díez, and M. V. Andrés, Laser Phys. Lett. **15**, 085113 (2018).
17. E. Hernández-Escobar, M. Bello-Jiménez, R. López-Estopier, A. Camarillo-Avilés, O. Pottiez, M. A. García-Ramírez, M. Durán-Sánchez, and M. V. Andrés, Laser Phys. **29**, 015101 (2018).
18. G. Ramírez-Meléndez, M. Bello-Jiménez, C. Cuadrado-Laborde, A. Díez, J. Cruz, A. Rodríguez-Cobos, R. Balderas-Navarro, and M. V Andrés, Opt. Eng. **55**, 036105 (2016).
19. E. Alcusa-Sáez, A. Díez, and M. V. Andrés, Opt. Express **24**, 4899 (2016).
20. B. Posadas-Ramírez, M. Durán-Sánchez, R. I. Álvarez-Tamayo, B. Ibarra-Escamilla, E. Bravo-Huerta, and E. A. Kuzin, Opt. Express **25**, 2560 (2017).
21. Q. Wang, T. Chen, B. Zhang, A. P. Heberle, and K. P. Chen, Opt. Lett. **36**, 3750 (2011).

Detailed References

1. X. H. Li, X. M. Liu, X. H. Hu, L. R. Wang, H. Lu, Y. S. Wang, and W. Zhao, "Long-cavity passively mode-locked fiber ring laser with high-energy rectangular-shape pulses in anomalous dispersion regime," Opt. Lett. **35**(19), 3249-3251 (2010).
2. J. Chen, D. F. Jia, Y. C. Wu, C. L. Wang, Z. Y. Wang, and T. X. Yang, "Passively mode-locked fiber laser with a sub-megahertz repetition rate," Chin. Phys. Lett. **28**(11), 114203 (2011).
3. B. N. Nyushkov, A. V. Ivanenko, S. M. Kobtsev, S. K. Turitsyn, C. Mou, L. Zhang, V. I. Denisov, and V. S. Pivtsov, "Gamma-shaped long-cavity normal-dispersion mode-locked Er-fiber laser for sub-nanosecond highenergy pulsed generation," Laser Phys. Lett. **9**(1), 59-67 (2012).
4. S. Boivinet, J.-B. Lecourt, Y. Hernandez, A. Fotiadi, M. Wuilpart, and P. Mégret, "All-fiber 1-µm PM mode-lock laser delivering picosecond pulses at Sub-MHz repetition rate," IEEE Photonics Technol. Lett. **26**(22), 2256-2259 (2014).
5. Z. Mingfei, S. Haiyue, L. Tongling, and H. Kun, "Ultra-low repetition rate gain-switched thulium-doped fibre laser at 2 µm," Quantum Electron. **47**(10), 877-881 (2017).
6. S. M. Ou, G. Y. Liu, L. Guo, Z. G. Zhang and Q. M. Zhang, "870 fs, 448 kHz pulses from an all-polarization-maintaining Yb-doped fiber laser with a nonlinear amplifying loop mirror," Appl. Opt. **57**(18), 5068-5071 (2018).
7. D. Jia, Y. Jin, X. Sun, Z. Li, Z., C. Ge, and Z. Wang, "Self-starting dual mode-locking Er-doped fiber laser with low repetition rate," In 2018 Asia Communications and Photonics Conference (ACP) (pp. 1-3). IEEE (2018).
8. Y. Zaouter, L. Daniault, M. Hanna, D. N. Papadopoulos, F. Morin, C. Hönninger, F. Druon, E. Mottay, and P. Georges, "Passive coherent combination of two ultrafast rod type fiber chirped pulse amplifiers," Opt. Lett. **37**(9), 1460-1462 (2012).
9. G. Sobon, P. Kaczmarek, A. Gluszek, J. Sotor, and K. M. Abramski, "µJ-level, kHz-repetition rate femtosecond fiber-CPA system at 1555 nm," Opt. Commun. **347**, 8-12 (2015).
10. Z. Zhao and Y. Kobayashi, "Ytterbium fiber-based, 270 fs, 100 W chirped pulse amplification laser system with 1 MHz repetition rate," Appl. Phys. Express **9**(1), 012701 (2016).
11. S. Han, H. Jang, S. Kim, Y. J. Kim, S. W. Kim, "MW peak power Er/Yb-doped fiber femtosecond laser amplifier at 1.5 µm center wavelength," Laser Phys. Lett. **14**, 080002 (2017).
12. K. J. Lee, D. I. Yeom, and B. Y. Kim, "Narrowband, polarization insensitive all-fiber acousto-optic tunable bandpass filter," Opt. Express **15**(6), 2987-2992 (2007).
13. C. Cuadrado-Laborde, M. Bello-Jiménez, A. Díez, J. L. Cruz, and M. V. Andrés, "Long-cavity all-fiber ring laser actively mode locked with an in-fiber bandpass acousto-optic modulator," Opt. Lett. **39**(1), 68-71 (2014).
14. G. Ramírez-Meléndez, M. Bello-Jiménez, O. Pottiez, and M. V. Andrés, "Improved all-fiber acousto-optic tunable bandpass filter," IEEE Photonics Tech. L. **29**(12), 1015-1018 (2017).
15. L. Huang, W. Zhang, Y. Li, H. Han, X. Li, P. Chang, F. Gao, G. Zhang, L. Gao, and T. Zhu, "Acousto-optic tunable bandpass filter based on acoustic-flexural-wave-induced fiber birefringence," Opt. Lett. **43**(21), 5431-5434 (2018).
16. M. Bello Jiménez, E. Hernández Escobar, A. Camarillo Avilés, O. Pottiez, A. Díez, and M. V. Andrés, "Actively mode-locked all-fiber laser by 5 MHz transmittance modulation of an acousto-optic tunable bandpass filter," Laser Phys. Lett. **15**(8), 085113 (2018).
17. E. Hernández-Escobar, M. Bello-Jiménez, R. López-Estopier, A. Camarillo-Avilés, O. Pottiez, M. A. García-Ramírez, M. Durán-Sánchez, and M. V. Andrés, "Q-switching and mode locking pulse generation from an all-fiber ring laser by intermodal acousto-optic bandpass modulation," Laser Phys. **29**(1), 015101 (2018).
18. G. Ramírez-Meléndez, M. Bello-Jiménez, C. Cuadrado-Laborde, A. Díez, J. Cruz, A. Rodríguez-Cobos, R. Balderas-Navarro y M. V Andrés, Acousto-optic Interaction in Biconical Tapered Fibers: Shaping of the Stopbands," Opt. Eng. **55**(3), 036105 (2016).
19. E. Alcusa-Sáez, A. Díez, and M. V. Andrés, "Accurate mode characterization of two-mode optical fibers by in-fiber acousto-optics," Opt. Express **24**(5), 4899-4905 (2016).
20. B. Posada-Ramírez, M. Durán-Sánchez, R. I. Álvarez-Tamayo, B. Ibarra-Escamilla, E. Bravo-Huerta, and E. A. Kuzin, "Study of a Hi-Bi FOLM for tunable and dual-wavelength operation of a thulium-doped fiber laser," Opt. Express **25**(3), 2560 -2568 (2017).
21. Q. Wang, T. Chen, B. Zhang, A. P. Heberle, and K. P. Chen, "All-fiber passively mode-locked thulium-doped fiber ring oscillator operated at solitary and noiselike modes," Opt. Lett. **36**(19), 3750-3752 (2011).